Supporting Information

Deciphering the Work Function Induced Local Charge Regulation towards Activating Octamolybdate Cluster-based Solid for Acidic Water Oxidation

Harshita Bagdwal,[a] Parul Sood,[a] Arshminder Kaur Dhillon,[a] Ashi Singh,[b] and Monika Singh*[a]

[a] Institution: Institute of Nano Science and Technology
Address: Knowledge City, Sector-81, Mohali
[b] Department of Chemistry, Indian Institute of Technology, Delhi

E-mail: monika@inst.ac.in

Table of Contents

Section 1. Experimental section

All the solvents and reagents used were acquired of the highest purity and are commercially available. They are used as such without any extra purification.

1.1 Synthesis of {$Cu(pz)_4\}_2Mo_8O_{26}]\cdot 2H_2O$ (named as Cat 1)

Initially, Ammonium molybdate tetrahydrate (1 mmol) is treated with $CuCl_2.2H_2O$ (1.5 mmol) in 20 mL of water. Further pyrazole (1 mmol) is added to it and kept stirring for 2 hours. The mixture is carefully poured into a **50-milliliter Teflon container** and heated to 140º C for 72 hours. After the completion, the reaction is cooled down to room temperature. The filtered solution is set aside for crystallization at **ambient temperature**. Blue color crystals were obtained after 2-3 days.

1.2 Synthesis of rGO

Graphene oxide was synthesized by the known reported technique.[1] Dried graphene oxide (GO) powder, placed on a crucible, underwent thermal treatment in a already heated muffle furnace at 350°C for 30 seconds. It's imperative to extract the crucible from the furnace gradually to avoid material loss, as the pressure variance could lead to dispersion of the material into the atmosphere. The resultant substance obtained after this process was a black powder, referred to as reduced graphene oxide (rGO).[2]

1.3 Synthesis of Nanocomposite

The composite is formed by 15 minutes of mechanical grinding of Cat 1 and reduced graphene oxide. The obtained crystal of Cat 1 is powdered and mixed with rGO { 1:1 (15mg:15mg) , 2:1 (30mg:15mg), 4:1 (60 mg:15mg) respectively} followed by mechanical grinding for 15 mins using mortar and pestle.

Section 2. Physical Characterization

Powder X-ray diffraction (PXRD) studies were carried out on a Bruker D8 – Advance Eco X-ray Diffractometer with Cu-Kα radiation (1.5418 Å). The morphological analysis of the catalyst was done by using a scanning electron microscope (SEM) from JEOL (JSM IT-300) provided with an energy-dispersive X-ray diffractometer (Bruker) and transmission electron microscopy (TEM). Valence states of the elements were found by X-ray photoelectron Spectroscopy (XPS) spectrometer (K-Alpha 1063).

Section 3. Electrochemical Study

All the electrochemical measurements were performed on the Metrohm-Autolab electrochemical workstation. A conventional three-electrode setup is used with a graphite electrode as the counter electrode, and an Ag/AgCl (3M KCl) electrode as a reference electrode. The ink for coating the graphitic strip as working electrode was prepared by taking 5 mg of catalyst in 500 μL of ethanol and 20 μL of 5 wt% nafion. The area of the sample when performing the electrochemical study was 0.5cm * 0.5cm. The mixture was sonicated for 2-3 hours to make a homogeneous mixture and then 100 μL of the ink was coated on the graphitic strip. All the data was collected in 0.5 M H_2SO_4. The equation used for the conversion to a Reversible Hydrogen electrode is $E_{RHE} = E_{Ag/AgCl} + 0.197 + 0.059*pH$. The determination of Tafel slope was done by fitting the linear region of the Tafel plot into the Tafel equation: 4

$$\eta = b \log(j) + a$$

The double layer capacitance (Cdl) was calculated by taking the CV scans in a non-Faradaic potential range of as-prepared catalysts electrodes in 0.5 M H_2SO_4 at a scan rate of 10 to 60 mV/s.

ECSA was determined by using the equation ECSA = Cdl/Cs

To check the stability of the catalyst, the chronoamperometric experiment was performed for more than 24 hours at the higher current density of 100 mA/cm^2. All the electrochemical data was recorded at room temperature.

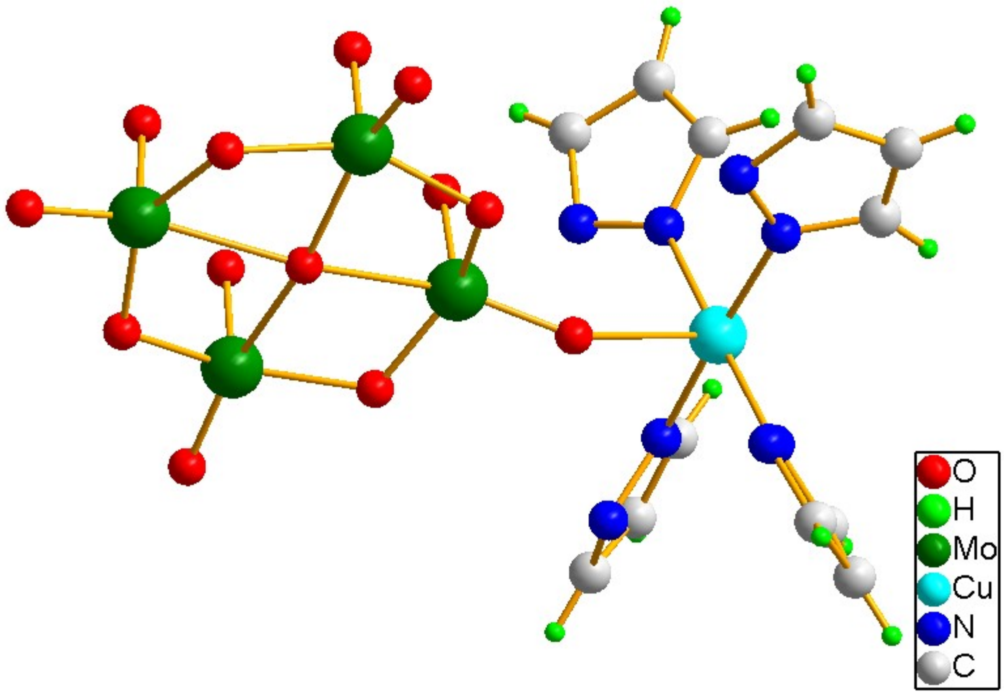

Fig. S1. Asymmetric Unit of Cat 1.

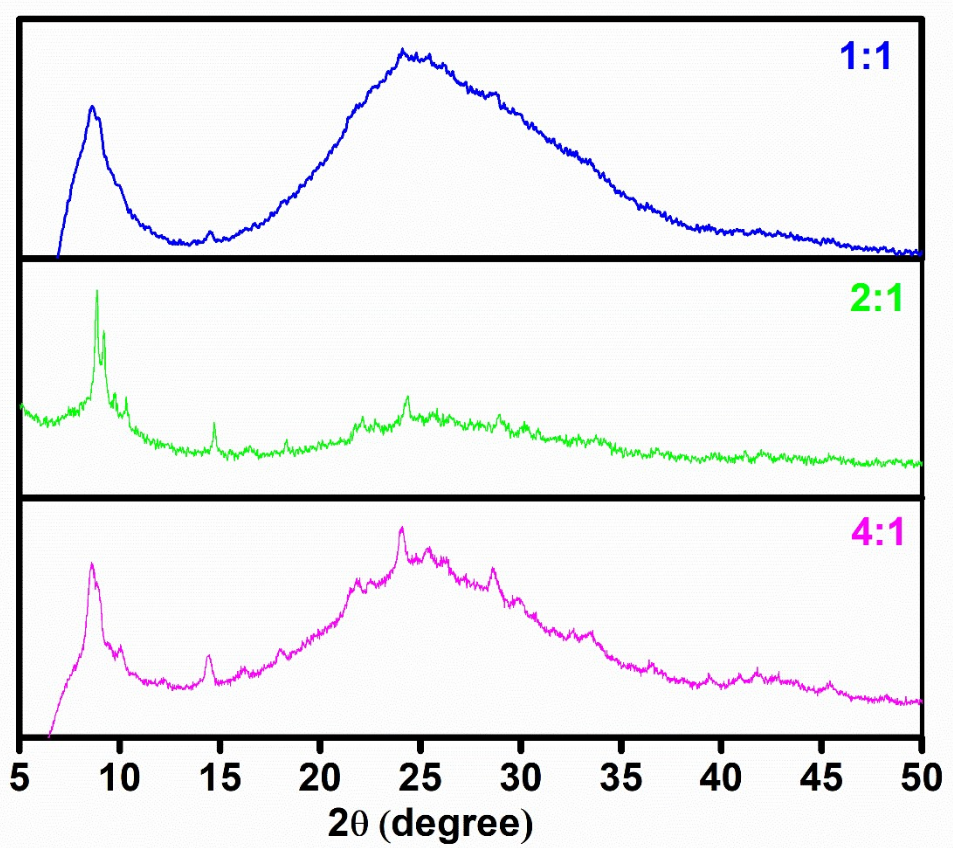

Fig. S2. XRD plot for 1:1, 2:1, and 4:1.

Table S1. Comparison table with reported acidic OER catalysts

S.No.	Material/Working electrode	Electrolyte	Overpotential @10mA/cm^2 (mV)	Tafel Slope (mV/dec)	Stability (hours)	Reference
1	Mn-RuO2	0.5 M H_2SO_4	143	40	480	[3]
2	(Ru–W)Ox	0.5 M H_2SO_4	170	46.2	300	[4]

3	Sr–Ru–Ir	0.5 M H_2SO_4	190	39	150 hrs@ 1mA/cm^2	[5]
4	1T-IrO2	0.5 M H_2SO_4	197	49	45 hrs@ 50mA/cm^2	[6]
5	$RuCoO_x$	0.1 M $HClO_4$	200	50.1	100	[7]
6	Ni-RuO2	0.1 M $HClO_4$	214	42.6	200	[8]
7	AD-HN-Ir	0.5 M H_2SO_4	216	39	100	[9]
8	Ru_5W_1Ox	0.5 M H_2SO_4	235	42	24	[10]
9	IrOxQD/GDY	0.5 M H_2SO_4	236	70	20	[11]
10	$Ir_{1-x}(Ir_{0\cdot8}V_{0\cdot2}O_2)_x$-BHC	0.1 M HClO4	238	39.87	130	[12]
11	COOH-MWNTs	0.5 M H_2SO_4	265	82	10	[13]
12	$Mn_{7.5}O_{10}Br_3$	0.5 M H_2SO_4	295	68	500	[14]
13	RuIr@CoNC	0.5 M H_2SO_4	300	45	40	[15]
14	**POM-rGO (2:1) nanocomposite**	**0.5 M H_2SO_4**	**185**	**252**	**24**	**Current work**

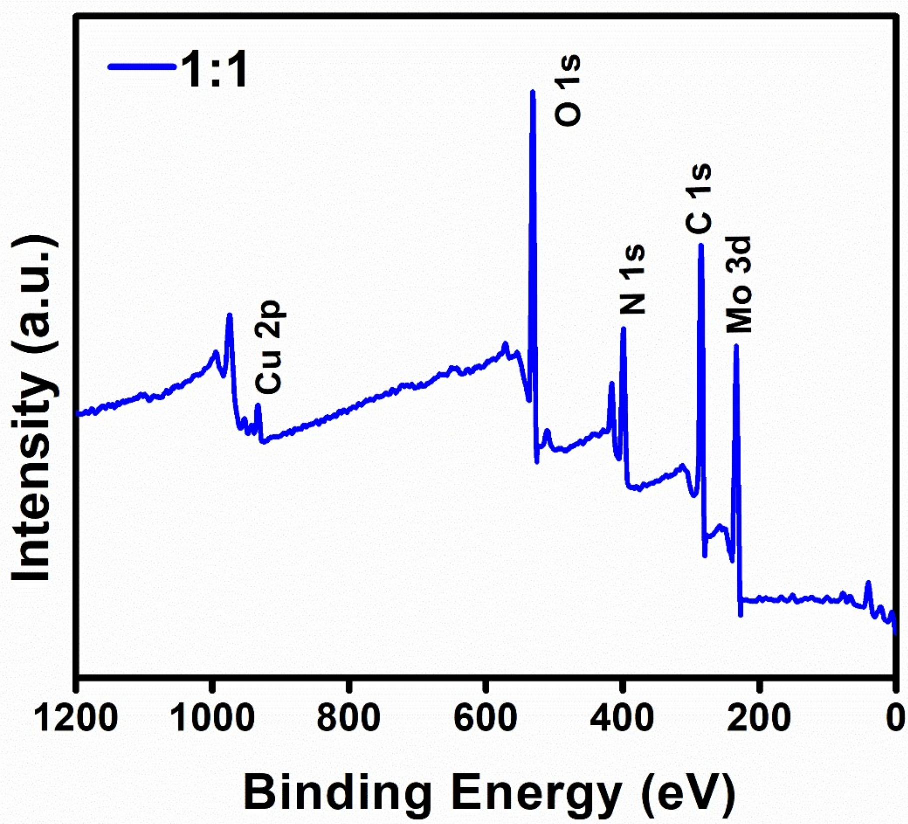

Fig. S3. XPS survey spectra of 1:1 POM-rGO nanocomposite.

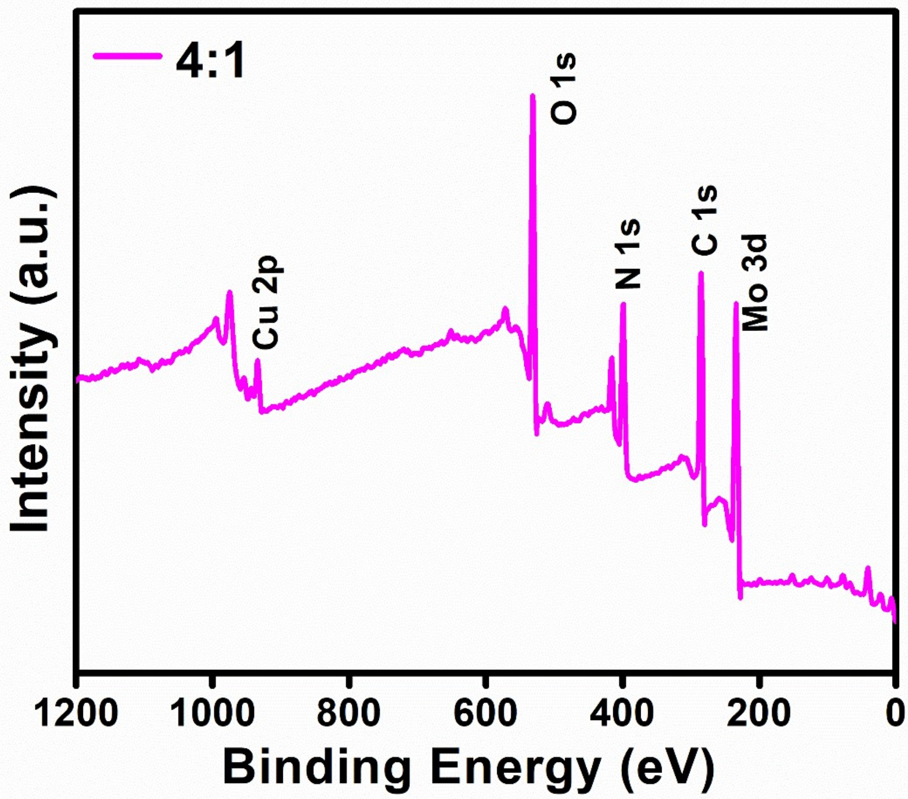

Fig. S4. XPS survey spectra of 4:1 POM-rGO nanocomposite.

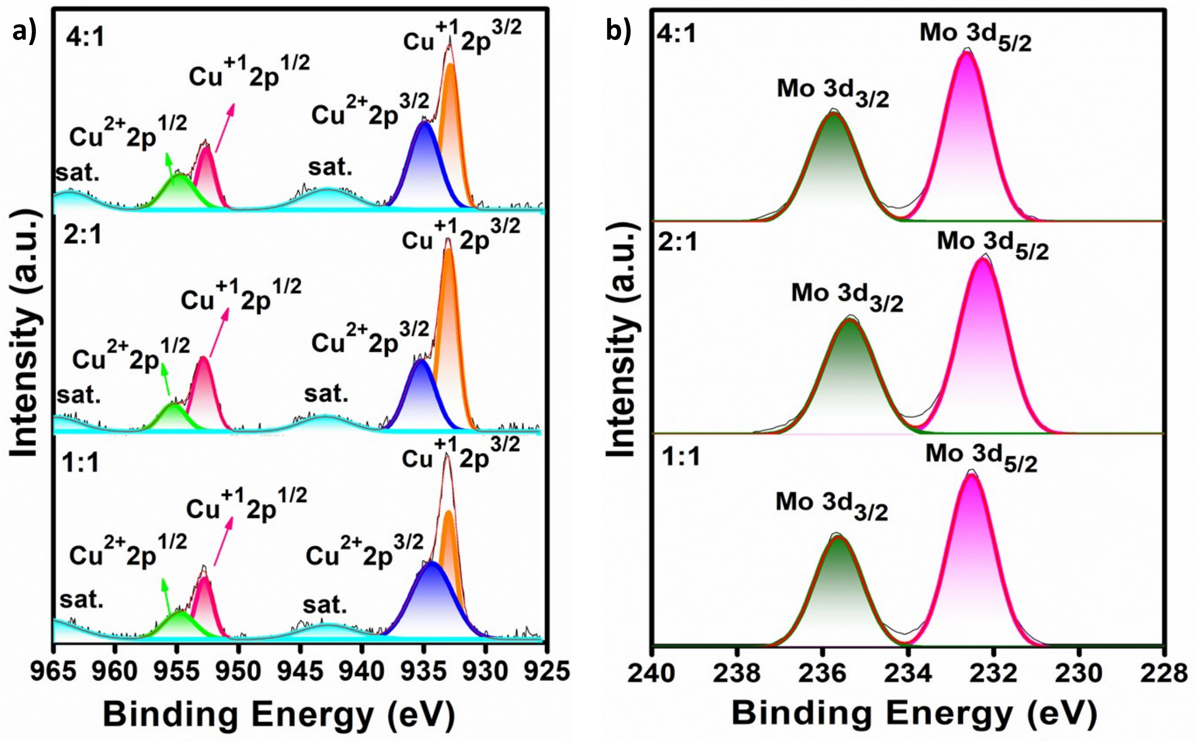

Fig. S5. Comparative High-resolution XPS spectra of (a) Cu 2p, (b) Mo 3d of 1:1, 2:1 and 4:1 nanocomposite

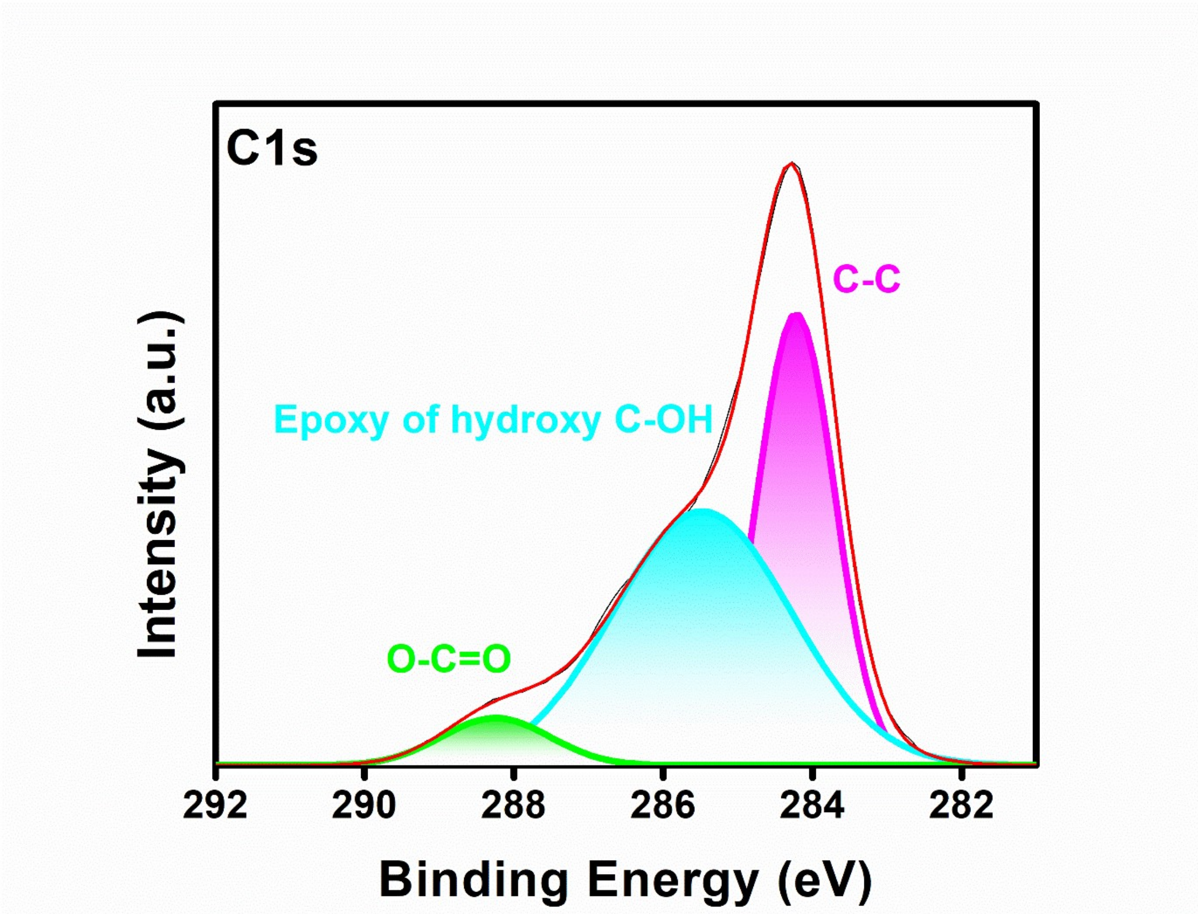

Fig. S6. High resolution C1s spectra for 2:1 nanocomposite.

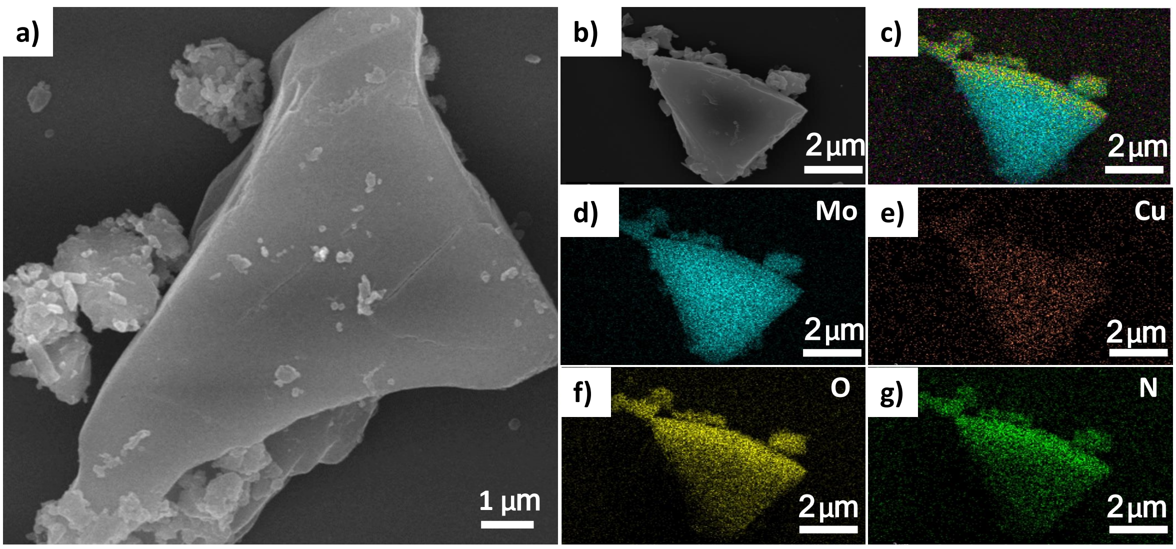

Fig. S7. FESEM image and elemental mapping of Cat 1.

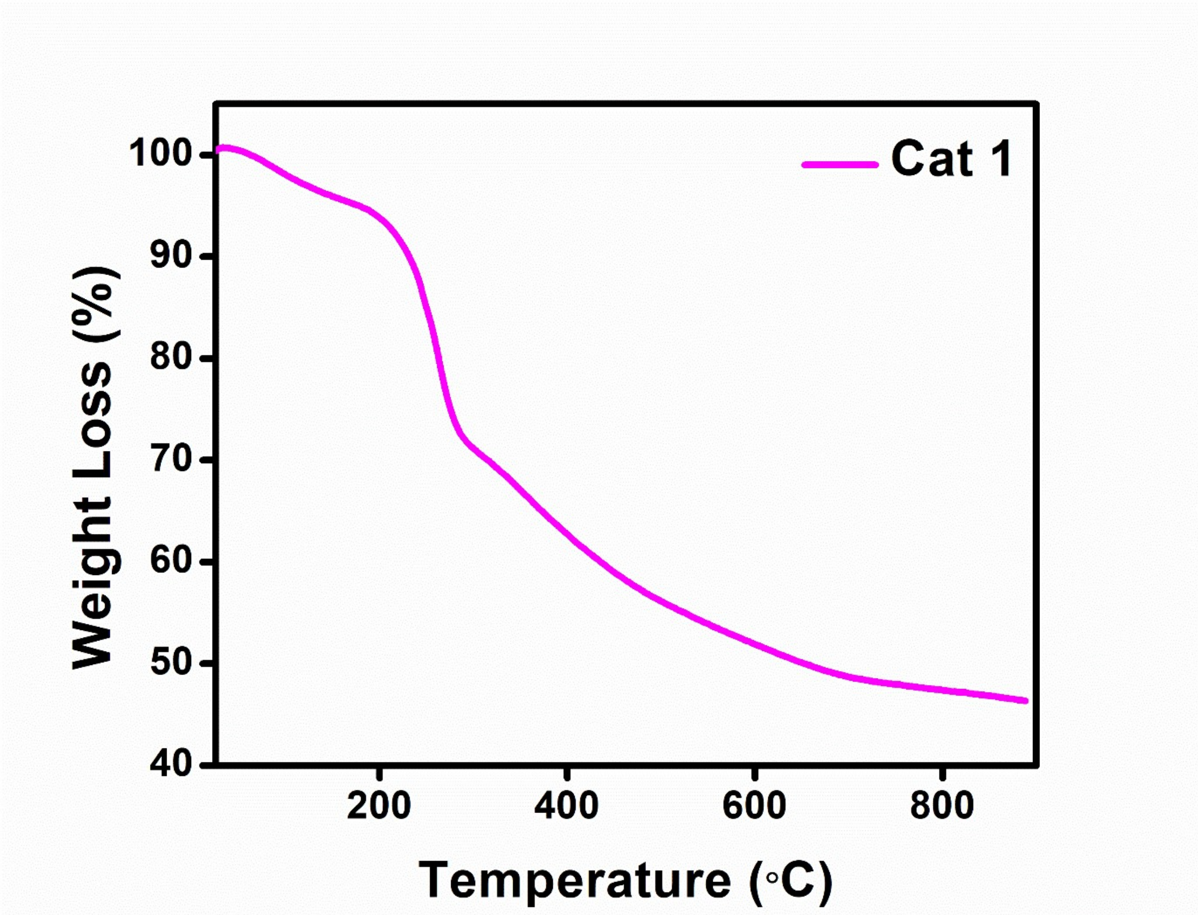

Fig. S8. Thermogravimetric analysis (TGA) curve of Cat 1.

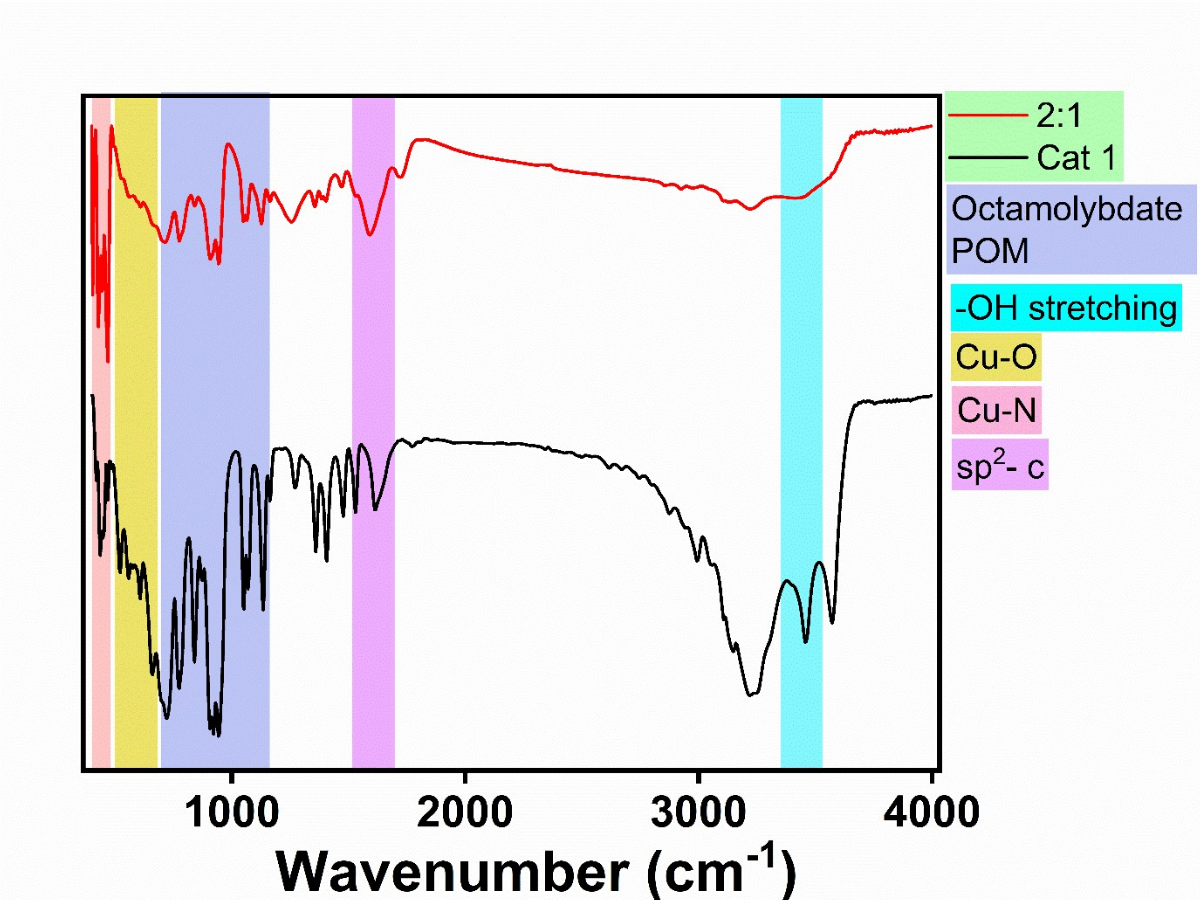

Fig. S9. FTIR spectra of Cat 1 and 2:1 nanocomposite.

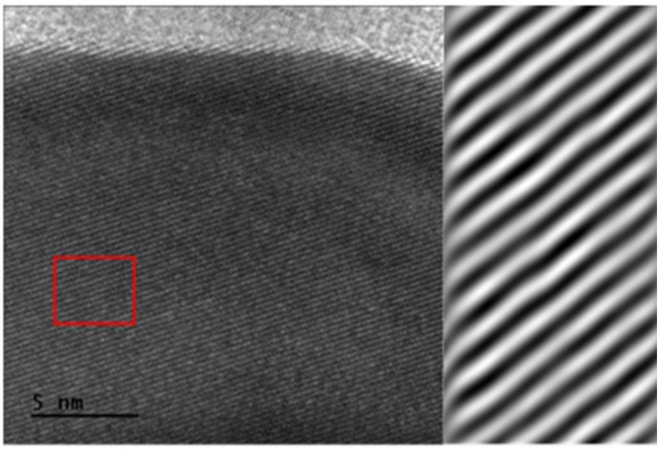

Fig. S10. HRTEM of 2:1 before OER test.

Table S2. Comparison of OER performance and Work Function of Cat 1 and composites of Cat 1 and rGO in different ratios.

Catalysts	**Overpotential(mV) @ 10mA/cm²**	**Work Function**
Cat. 1	365	4.49
Cat. 1 & rGo (1:1)	346	4.14
Cat. 1 & rGo (2:1)	185	1.74
Cat. 1 & rGo (4:1)	397	4.63

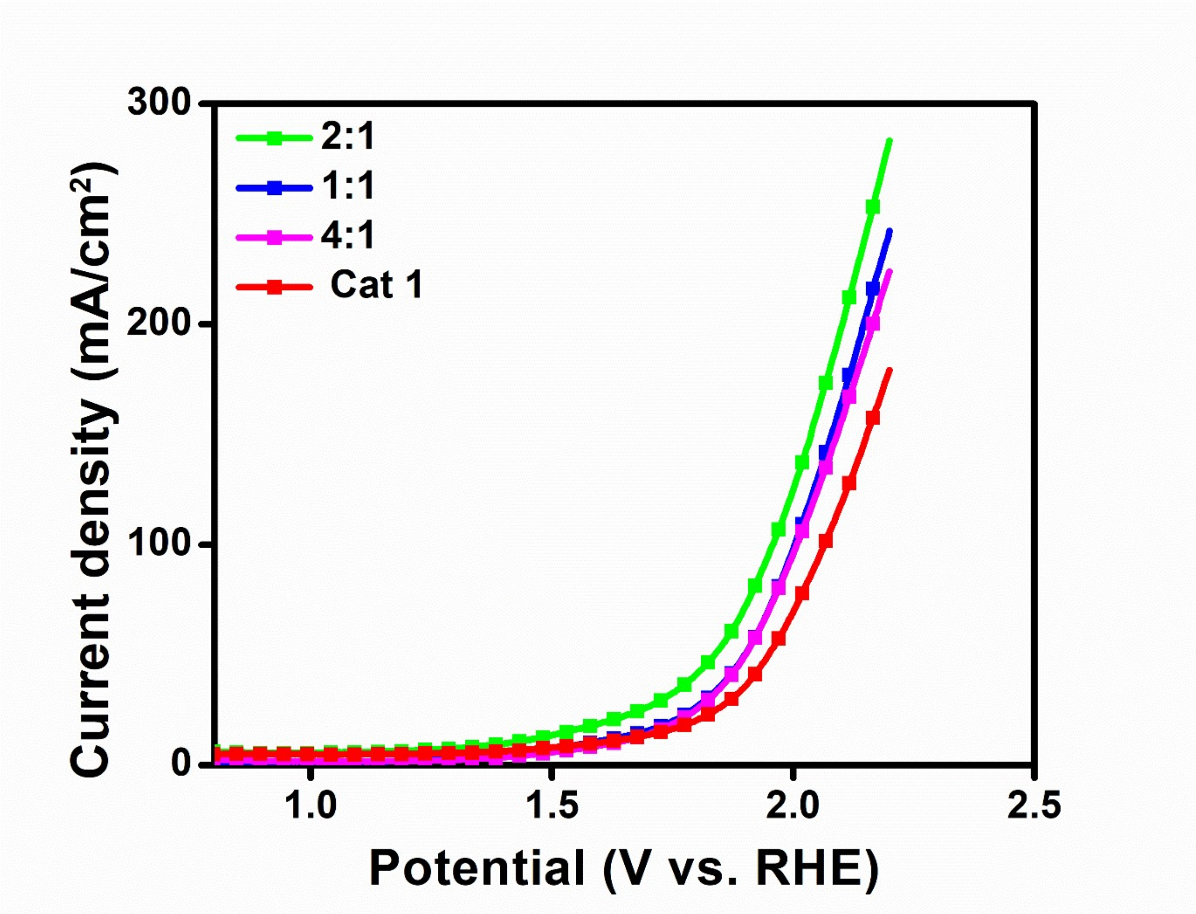

Fig. S11. LSV curves of Cat 1 & rGO composite in different ratios.

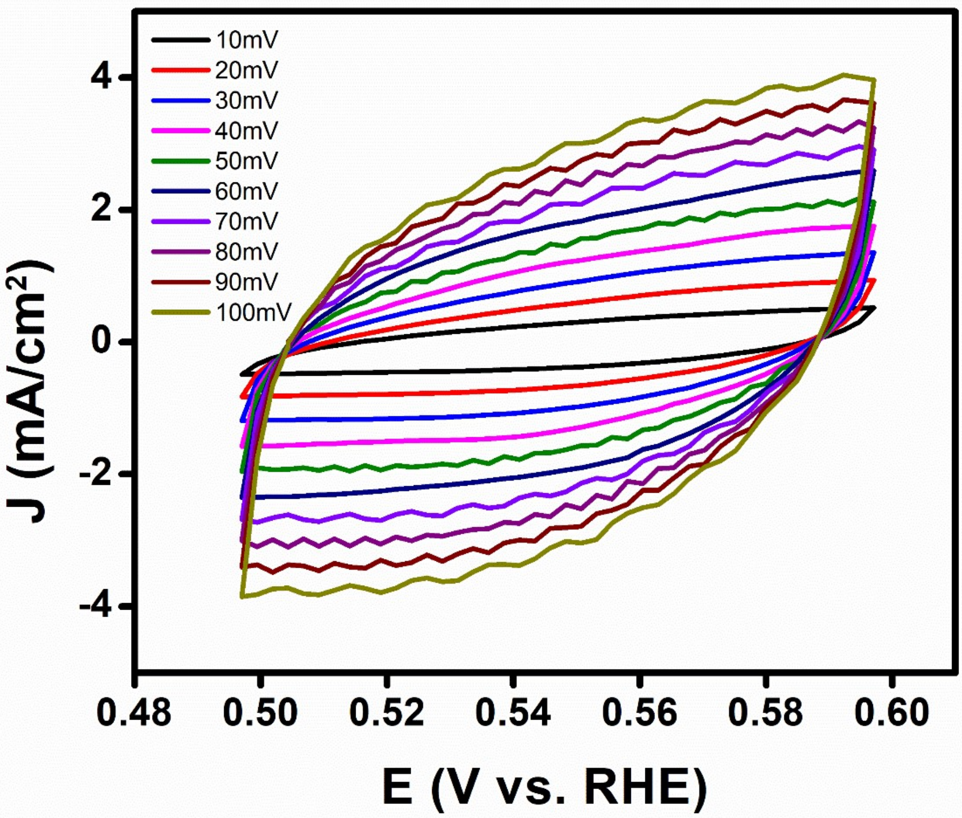

Fig. S12. CV cycles for Cat 1 at different scan rates.

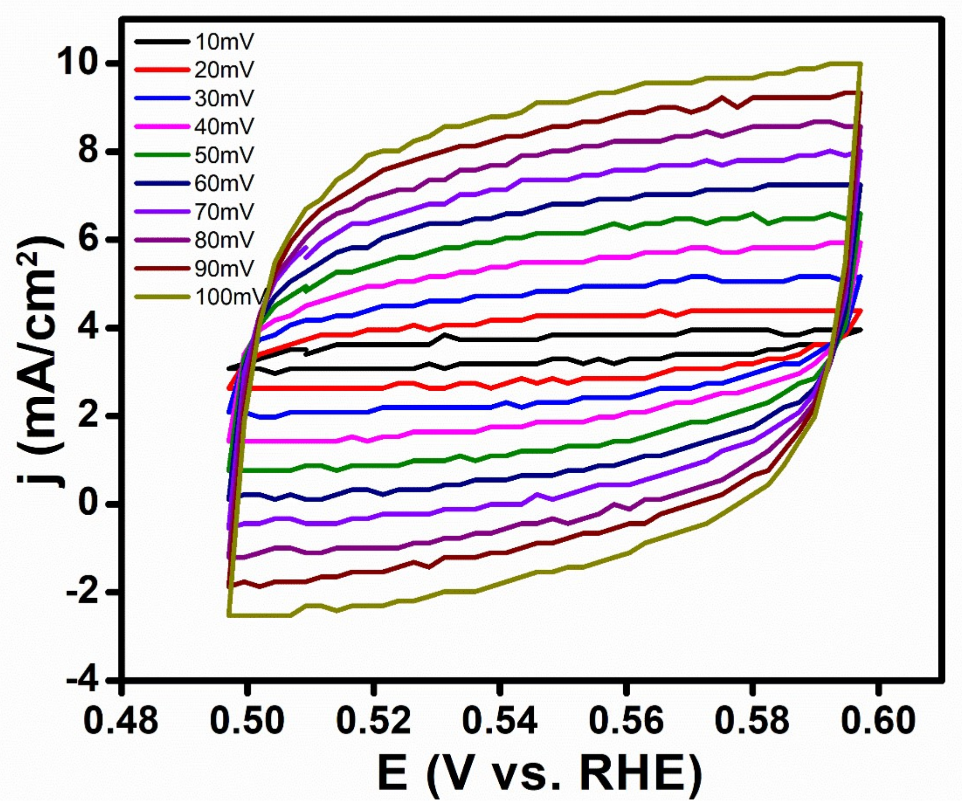

Fig. S13. CV cycles for Cat 1 & rGO (2:1) at different scan rates.

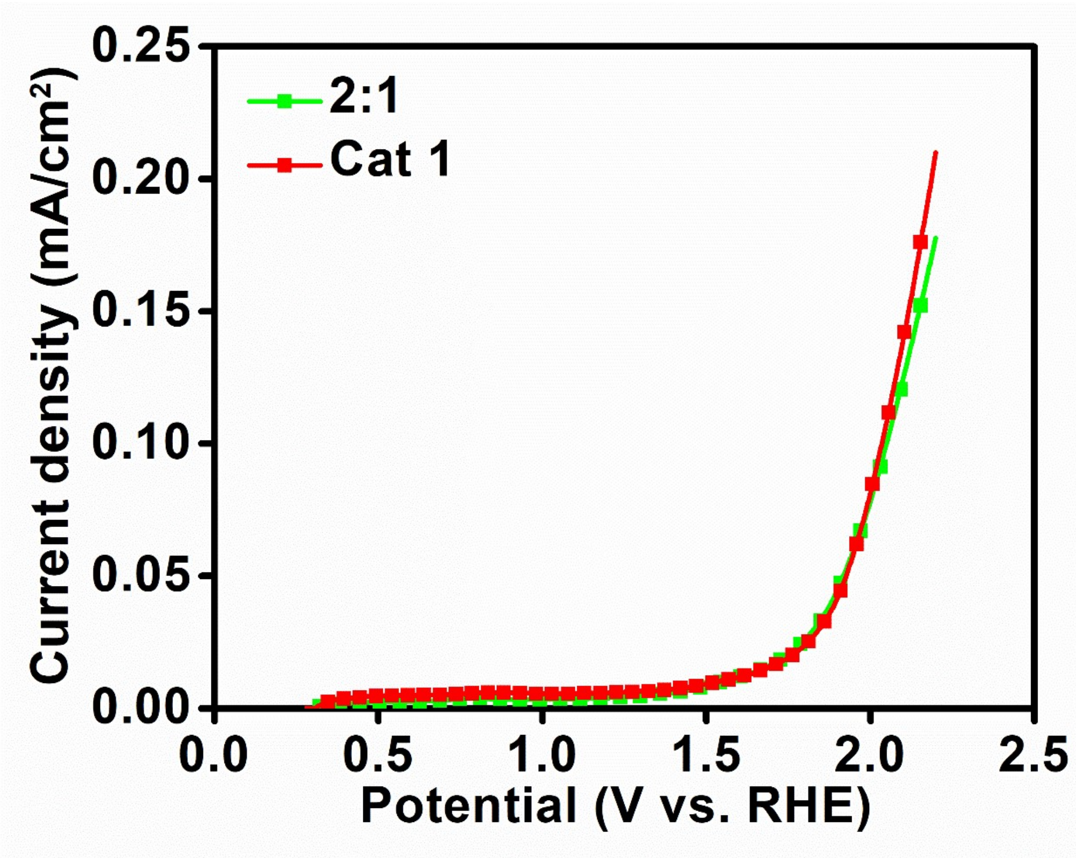

Fig. S14. ECSA normalized LSV of 2:1 and Cat 1.

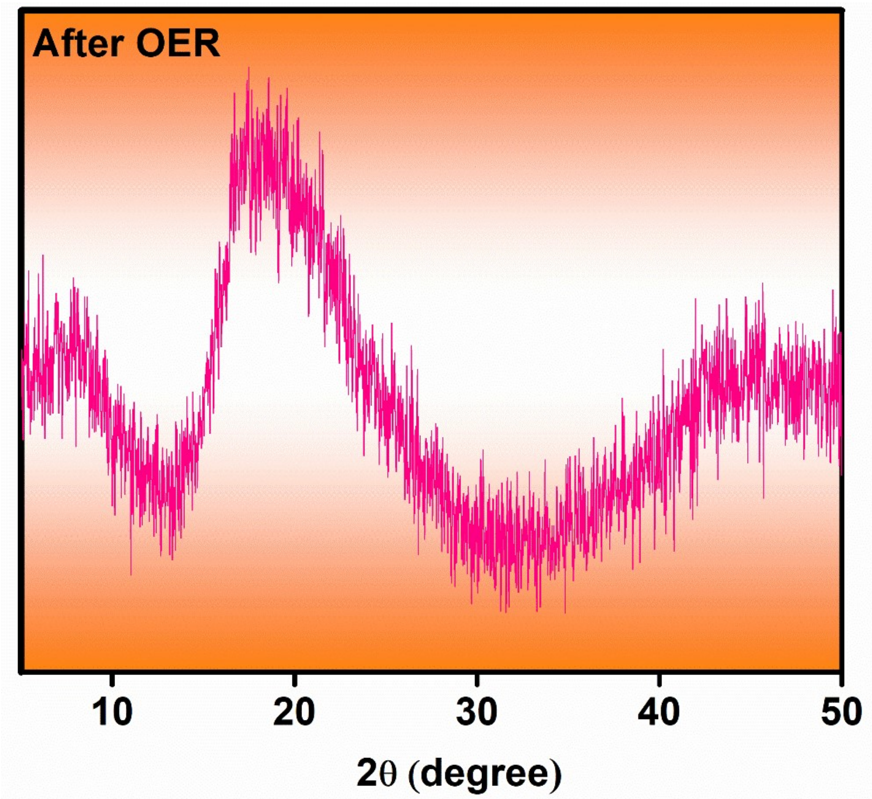

Fig. S15. Post OER PXRD pattern for 2:1 nanocomposite.

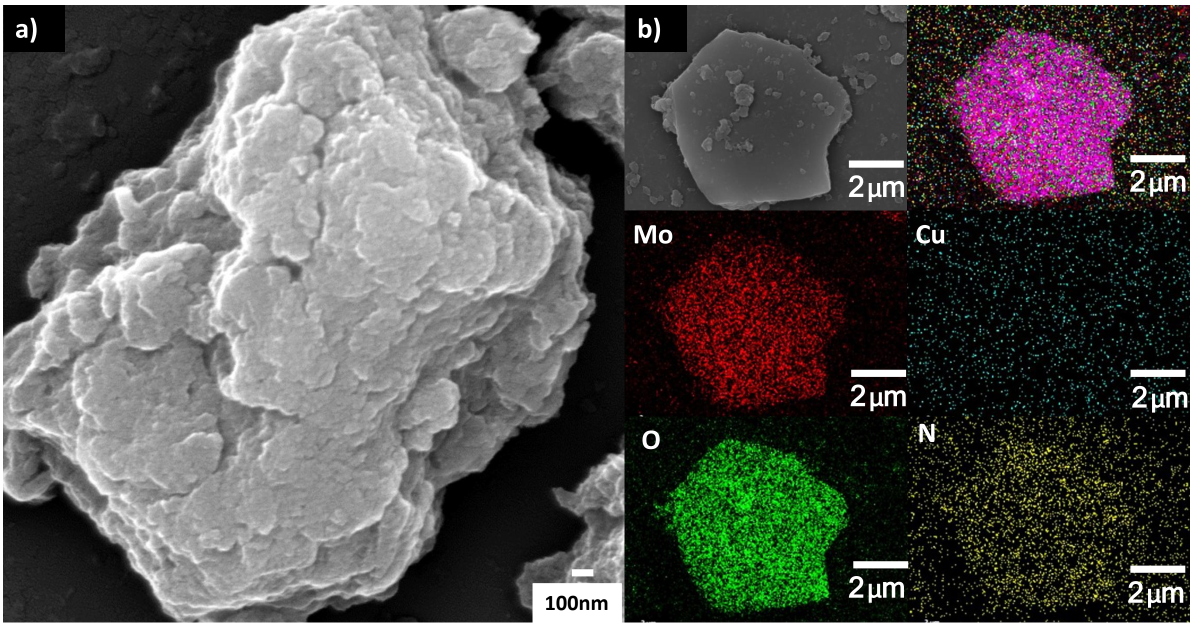

Fig. S16. Post OER (a) FESEM micrographs of 2:1 nanocomposite, (b) elemental mapping.

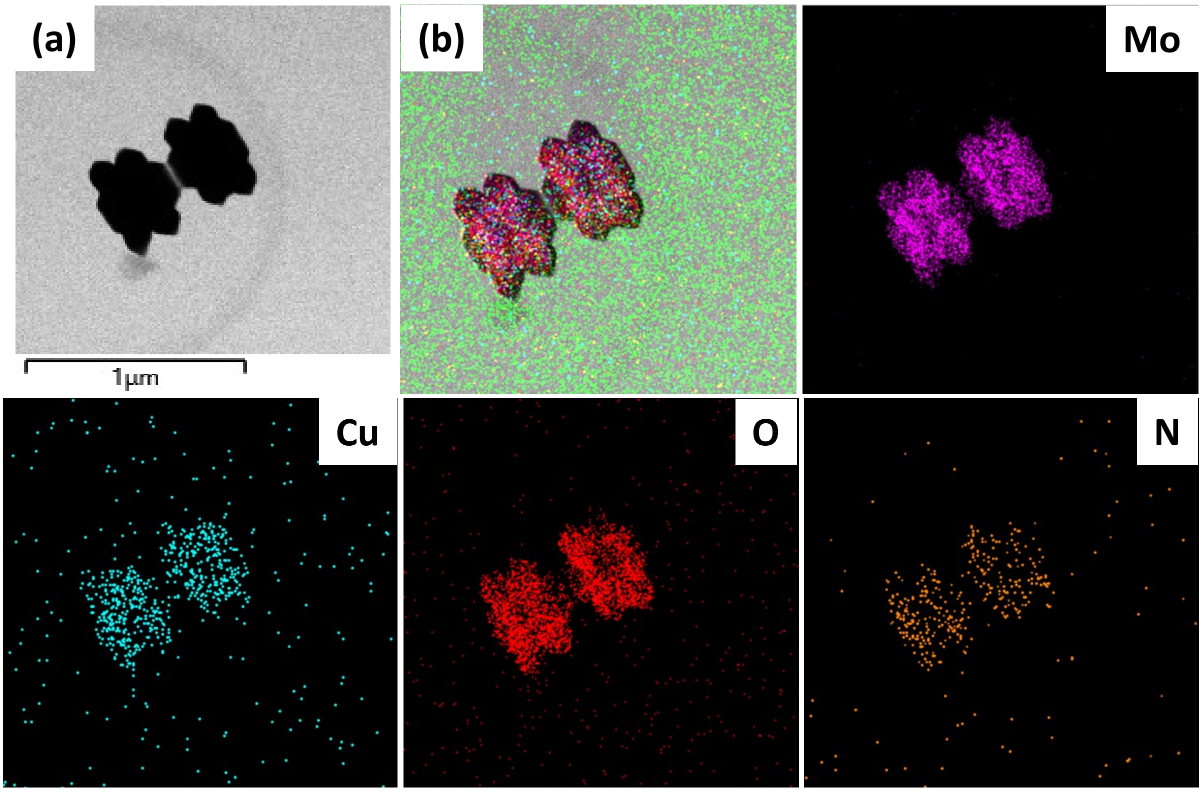

Fig. S17. Post OER element mapping of 2:1 nanocomposite.

References

1 S. N. Alam, N. Sharma and L. Kumar, *Graphene*, 2017, **6**, 1–18.
2 A. E. F. Oliveira, G. B. Braga, C. R. T. Tarley and A. C. Pereira, *J Mater Sci*, 2018, **53**, 12005–12015.
3 L. Li, J. Zhou, X. Wang, J. Gracia, M. Valvidares, J. Ke, M. Fang, C. Shen, J.-M. Chen, Y.-C. Chang, C.-W. Pao, S.-Y. Hsu, J.-F. Lee, A. Ruotolo, Y. Chin, Z. Hu, X. Huang and Q. Shao, *Advanced Materials*, 2023, **35**, 2302966.
4 L. Deng, S.-F. Hung, Z.-Y. Lin, Y. Zhang, C. Zhang, Y. Hao, S. Liu, C.-H. Kuo, H.-Y. Chen, J. Peng, J. Wang and S. Peng, *Advanced Materials*, 2023, **35**, 2305939.
5 Y. Wen, P. Chen, L. Wang, S. Li, Z. Wang, J. Abed, X. Mao, Y. Min, C. T. Dinh, P. D. Luna, R. Huang, L. Zhang, L. Wang, L. Wang, R. J. Nielsen, H. Li, T. Zhuang, C. Ke, O.

Voznyy, Y. Hu, Y. Li, W. A. Goddard III, B. Zhang, H. Peng and E. H. Sargent, *J. Am. Chem. Soc.*, 2021, **143**, 6482–6490.

6 Q. Dang, H. Lin, Z. Fan, L. Ma, Q. Shao, Y. Ji, F. Zheng, S. Geng, S.-Z. Yang, N. Kong, W. Zhu, Y. Li, F. Liao, X. Huang and M. Shao, *Nat Commun*, 2021, **12**, 6007.

7 W. Zhu, F. Yao, K. Cheng, M. Zhao, C.-J. Yang, C.-L. Dong, Q. Hong, Q. Jiang, Z. Wang and H. Liang, *J. Am. Chem. Soc.*, 2023, **145**, 17995–18006.

8 Z.-Y. Wu, F.-Y. Chen, B. Li, S.-W. Yu, Y. Z. Finfrock, D. M. Meira, Q.-Q. Yan, P. Zhu, M.-X. Chen, T.-W. Song, Z. Yin, H.-W. Liang, S. Zhang, G. Wang and H. Wang, *Nat. Mater.*, 2023, **22**, 100–108.

9 H. Su, W. Zhou, W. Zhou, Y. Li, L. Zheng, H. Zhang, M. Liu, X. Zhang, X. Sun, Y. Xu, F. Hu, J. Zhang, T. Hu, Q. Liu and S. Wei, *Nat Commun*, 2021, **12**, 6118.

10 Y. Wen, C. Liu, R. Huang, H. Zhang, X. Li, F. P. García de Arquer, Z. Liu, Y. Li and B. Zhang, *Nat Commun*, 2022, **13**, 4871.

11 Z. Wang, Z. Zheng, Y. Xue, F. He and Y. Li, *Advanced Energy Materials*, 2021, **11**, 2101138.

12 W. Ahmad, Y. Hou, R. Khan, L. Wang, S. Zhou, K. Wang, Z. Wan, S. Zhou, W. Yan, M. Ling and C. Liang, *Small Methods*, 2023, **7**, 2201247.

13 X. Zhang, W. Zhang, J. Dai, M. Sun, J. Zhao, L. Ji, L. Chen, F. Zeng, F. Yang, B. Huang and L. Dai, *InfoMat*, 2022, **4**, e12273.

14 S. Pan, H. Li, D. Liu, R. Huang, X. Pan, D. Ren, J. Li, M. Shakouri, Q. Zhang, M. Wang, C. Wei, L. Mai, B. Zhang, Y. Zhao, Z. Wang, M. Graetzel and X. Zhang, *Nat Commun*, 2022, **13**, 2294.

15 J. Xu, J. Li, Z. Lian, A. Araujo, Y. Li, B. Wei, Z. Yu, O. Bondarchuk, I. Amorim, V. Tileli, B. Li and L. Liu, *ACS Catal.*, 2021, **11**, 3402–3413.